Journal of Solid State Chemistry **152,** 353–360 (2000)
doi:10.1006/jssc.2000.8663, available online at http://www.idealibrary.com on IDEAL®

Metastable Hexagonal Vanadium Molybdate Study

Olivier Mougin,† Jean-Luc Dubois,‡ François Mathieu,† and Abel Rousset†,[1]

†*Laboratoire de Chimie des Matériaux Inorganiques et Energétiques, ESA CNRS 5070, Université Paul Sabatier—Bâtiment 2R1, 118, Route de Narbonne, 31062 Toulouse Cedex, France; and* ‡*Centre de Recherche et de Developpement de l'Est, Elf Atochem, BP 61005, 57501 Saint-Avold, France*

Received November 2, 1999; accepted February 24, 2000

The solid solution of vanadium in hexagonal molybdenum oxide has never previously been completely studied; no information has been given about the solubility limit or the thermal stability of the system. In this work, we have determined that the solubility limit is reached with the following composition: $(NH_4)_{0.13}V_{0.13}Mo_{0.87}O_3$. Our samples have been obtained by a soft chemistry method. The obtained precipitates have been processed and analyzed with several techniques. We have shown that the introduction of vanadium in the h-MoO_3 structure has several effects, on the thermal stability of the metastable mixed oxide, on the morphology, as well as on the lattice parameters. © 2000 Academic Press

Key Words: **vanadium; molybdenum; mixed oxide; solid solution; molybdate; hexagonal; metastable; MoO_3; thermal stability.**

1. INTRODUCTION

Different polymorphs of molybdenum trioxide are known: the orthorhombic structure α-MoO_3 (1, 2), and two metastable phases, β-MoO_3 (monoclinic) (3) and h-MoO_3 (hexagonal) (4). This last structure of molybdenum trioxide is recorded in the JCPDS file under the number 21-569. This is the only file for vanadium-free h-MoO_3 that has been recorded (5). We do not know anything about it, except that the X-ray diffraction analysis has been recorded from a sample given by Johnson Matthey Co., Ltd.. Its cell parameters are $a = 10.531$ Å and $c = 14.876$ Å, but no space group is specified.

Several reports have been published on the preparation of this hexagonal MoO_3 polymorph (4, 8–10). According to some of these authors, this phase contains monovalent cations (e.g., NH_4, K, Rb, Cs) in the large tunnels oriented along the *c*-axis of the hexagonal structure (Fig. 1).

The presence of this cation in the cavity of the hexagonal structure is necessary for the hexagonal structure to exist (4, 7, 8, 11, 12). The phase with the NH_4^+ cation, reported as hexagonal, is a partially dehydrated and deammoniated compound of composition $(NH_4)H_{6x-1}([\square_{Mo}]_xMo_{6-x})O_{18}$ (8, 12–15). In the 1998 JCPDS-ICDD files, no JCPDS card is reported for this compound.

The cation nature influences the lattice parameter values. We compared the results found in the literature (Table 1), and we observed that the presence or the nature of the cations in the structure's tunnels do not have an influence on the *c* parameter, but only on the *a* parameter. This can be explained by the fact that the cations in the tunnels have neighbors along the *a*- and *b*-axis, but not along the *c*-axis.

The preparation of Mo-containing compounds has been largely discussed and the existence of a phase $A_xMe_xMo_{1-x}O_3$ ($A = NH_4$, K, Rb, Cs; $Me =$ V, P, Sn, Ti, Zr, Si) with the hexagonal MoO_3 structure has been pointed out (4, 7, 11).

Because of its catalytic and electrochemical properties, the V–Mo–O system has already been studied and discussed (17–25). However, research must be performed on metastable phases, to determine their existence domain and their specific properties. This is the case, for instance, for the hexagonal molybdenum oxide (h-MoO_3) solid solutions for which the results are not consistent (7, 9, 11, 26–30). Most previous publications report the existence of phases $A_xV_xMo_{1-x}O_3$ ($A = K^+$, NH_4^+, Na^+), with $x = 0.13$ (7, 9, 11). No information is given about other compositions, and there are doubts regarding the existence of these phases for *x* bigger or smaller than 0.13. In these compounds, the cation's nature also influences the parameters *a* and *c* of the hexagonal lattice (Table 2).

Our objective is to show the existence, some properties, and the limits of this solid solution by using thermal analysis, X-ray analysis, electron microscopy, and infrared analysis.

2. SYNTHESIS PROCEDURE AND EXPERIMENTAL TECHNIQUES

Samples have been prepared via a soft chemistry method; we have precipitated V–Mo compounds by using 65%

[1]To whom correspondence should be addressed. E-mail: rousset@iris.ups-tlse.fr.

0022-4596/00 $35.00

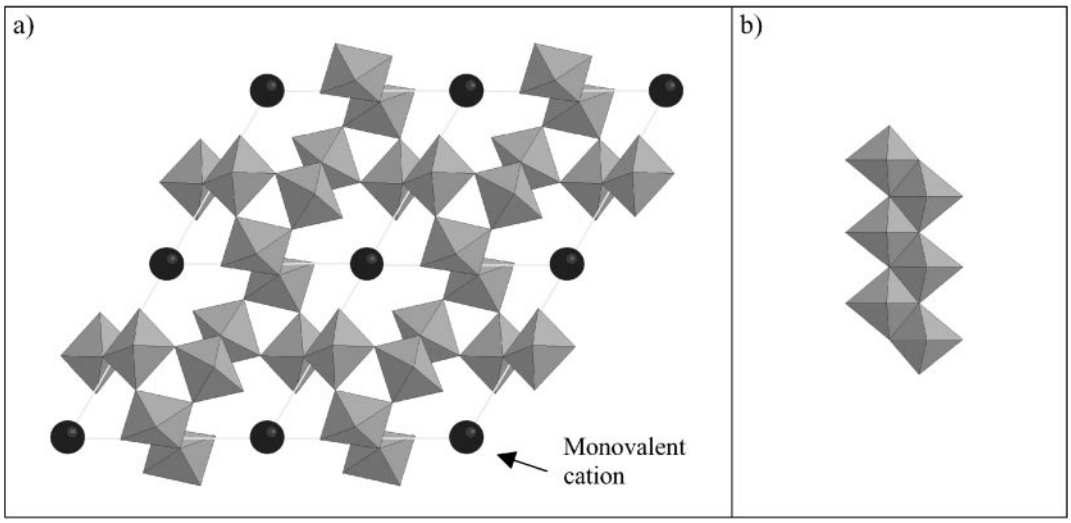

FIG. 1. (a) Projection (xy) of h-MoO_3 structure and (b) double chain of Mo octahedra along the c-axis (4).

nitric acid. A 500 ml aqueous solution with the appropriate concentration of ammonium heptamolybdate ([AHM] = 40.9–31.1 g/l) and ammonium metavanadate ([AMV] = 0–10.3 g/l) is introduced in 300 ml of nitric acid solution at pH 1 and $T = 70$–$80°C$. The pH is regulated and maintained at 1 during the complete step of introduction of AHM and AMV solution, by checking the pH every 5 minutes, and adding the appropriate quantity of HNO_3 (65%). At the end of the introduction, the system is steered during 2 hours at $T = 70$–$80°C$, filtered, and washed three times by dispersing the precipitate in 700 ml of ethanol (95% C_2H_5OH). The precipitate obtained is then dried in an oven at 70°C for 24 hours.

Elemental analysis was performed by atomic absorption spectrometry (Service Central d'Analyse, CNRS, Vernaison, France).

X-ray powder diffraction patterns were collected on a Siemens D501 diffractometer, equipped with a Peltier cooling effect Si(Li) detector, and using the Cu$K\beta$ radiation ($\lambda = 0.139326$ nm, i.e., an energy window centered on 8.9 keV). The whole apparatus is controlled by a DACO MP computing system. The diffraction patterns have been compared to the JCPDS file published in 1998 by the International Center for Diffraction Data (5).

The thermal stability has been evaluated by DTA–TG with a Setaram TG–DTA 92 instrument, in air flux with a 3°C/minute scan rate; during the thermal cycling, the gas emissions were observed by mass spectroscopy analysis, coupled to the DTA–TG.

The samples have also been observed by scanning electron microscopy (SEM) with a JEOL JSM 6400 microscope, and by transmission electron microscopy (TEM) with

TABLE 1
Comparison of the Parameters a and c of Several Molybdenum Oxides with the Hexagonal Structure, Containing Different Cations

Reference	Formula	a (Å)	c (Å)
JCPDS card 21-569	MoO_3	10.531	3.719
(12)	$(NH_4)_xMo_5O_{15}(OH)_x$, yH_2O	10.576	3.728
(13)	$Na\ H_{6x-1}Mo_{6-x}O_{18}$, $2H_2O$	10.595	3.722
	$KH_{6x-1}Mo_{6-x}O_{18}$	10.520	3.725
	$RbH_{6x-1}Mo_{6-x}O_{18}$	10.573	3.720
	$CsH_{6x-1}Mo_{6-x}O_{18}$	10.604	3.721
	$(NH_4)H_{6x-1}Mo_{6-x}O_{18}$	10.548	3.722
	$AgH_{6x-1}Mo_{6-x}O_{18}$, $2H_2O$	10.585	3.726
(14)	$KMo_5O_{15}OH.2H_2O$	10.550	3.727
(15)	$(NH_4)Mo_5O_{18}H_5$	10.58	3.726
(16)	$(NH_4)Mo_{5.3}O_{17.3}H_{1.7}$, $0.4H_2O$	10.569	3.721

TABLE 2
Comparison of the Parameters a and c of Several Vanadium–Molybdenum Oxides with the Hexagonal Structure, Containing Different Cations

Reference	Formula	a (Å)	c (Å)
JCPDS card 48-0766	$V_{0.13}Mo_{0.87}O_{2.935}$	10.592	3.699
JCPDS card 81-2414	$V_{0.12}Mo_{0.88}O_{2.94}$	10.593	3.694
(4)	$(NH_4)_xV_xMo_{1-x}O_3$ $x = 0, 2$	10.54	3.71
(7)	$V_{0.13}Mo_{0.87}O_{2.935}$	10.593	3.694
	$K_{0.13}V_{0.13}Mo_{0.87}O_3$	10.481	3.701
	$Rb_{0.13}V_{0.13}Mo_{0.87}O_3$	10.523	3.698
	$Cs_{0.13}V_{0.13}Mo_{0.87}O_3$	10.617	3.694
(9)	$H_{0.13}V_{0.13}Mo_{0.87}O_3$, $0.26H_2O$	10.583	3.698
	$V_{0.13}Mo_{0.87}O_{2.935}$	10.56	3.695
(11)	$K_{0.13}V_{0.13}Mo_{0.87}O_3$	10.481	3.701
(29)	$(NH_4)_{0.2}V_{0.2}Mo_{0.8}O_3$	10.531	3.719
(30)	$Na_{0.13}V_{0.13}Mo_{0.87}O_3$, nH_2O	10.628	3.697

a JEOL 2010 TEM microscope. The local metal content and the particle composition have been investigated by TEM energy dispersive X-ray (EDX) microanalysis.

3. RESULTS AND DISCUSSION

The samples obtained by the soft chemistry method described above have been analyzed for vanadium and molybdenum content by atomic absorption spectrometry; the results have been expressed as V_xMo_{1-x} (Table 3), where Δx represents the precision on the x value.

The precipitated samples have the peculiarity of being well-crystallized without the need of any additional processing (Fig. 2). The structure of these samples is hexagonal, h-MoO_3 like. This result is not consistent with that of Tatibouet and Germain (10); by precipitating a hot aqueous solution of ammonium heptamolybdate with nitric acid, and drying the precipitate at 110°C, they found that the powder obtained is amorphous. By heating the powder at 210°C, they obtained the hexagonal MoO_3, which transforms into the orthorhombic form over 340°C.

On our side, we observed that the precipitate is well crystallized, and presents a diffraction pattern corresponding to the h-MoO_3 JCPDS card (Table 4). For x greater than 0.18, diffraction patterns show the presence of another phase, not very well crystallized, corresponding to $V_9Mo_6O_{40}$ (Fig. 2).

The samples have been observed by scanning electron microscopy and transmission electron microscopy (Figs. 3 and 4). Two kinds of morphology are observed:

— For $x < 0.18$, the precipitate has a unique needle morphology, and the section of these needles is hexagonal.

— For $x > 0.18$, a second morphology appears in addition to the needles, which could correspond to the $V_9Mo_6O_{40}$ phase observed by X-ray diffraction.

Therefore, we can assume that the V–Mo hexagonal solid solution has a needle morphology oriented along the c-axis of the hexagonal structure. We tried to confirm this hypothesis by electron diffraction experiments, but the needles did not resist to high power of the electron beam.

According to the SEM photographs (Fig. 3), one can say that the presence of vanadium influences the dimensions of

TABLE 3
Compositions of the Studied Samples, Expressed in V_xMo_{1-x} Form

Compositions	Δx
Mo	0.000
$V_{0.01}Mo_{0.99}$	0.001
$V_{0.02}Mo_{0.98}$	0.001
$V_{0.03}Mo_{0.97}$	0.001
$V_{0.05}Mo_{0.95}$	0.002
$V_{0.08}Mo_{0.92}$	0.003
$V_{0.09}Mo_{0.91}$	0.004
$V_{0.12}Mo_{0.88}$	0.005
$V_{0.13}Mo_{0.87}$	0.005
$V_{0.15}Mo_{0.85}$	0.006

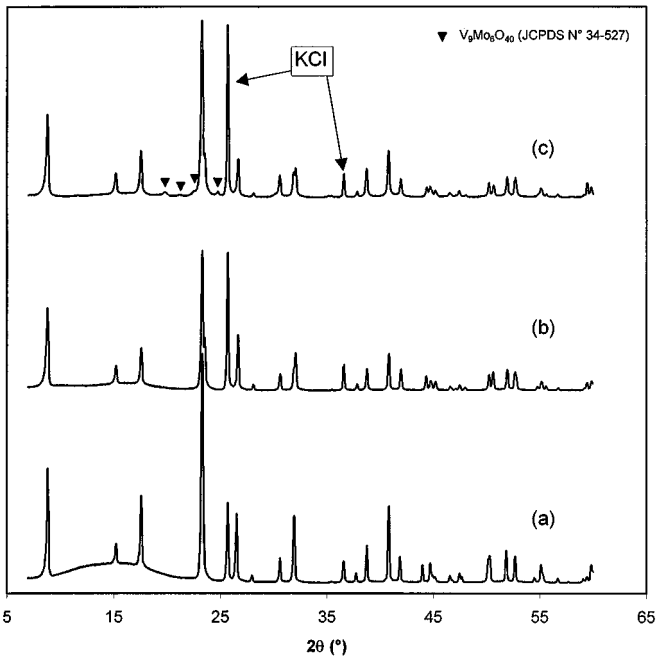

FIG. 2. XRD of well-crystallized powders, with the hexagonal structure, obtained by soft chemistry with different proportions of vanadium: (a) vanadium-free, (b) 12% vanadium, and (c) 18% vanadium.

TABLE 4
Experimental and Theoretical Data for h-MoO_3

hkl	d_{JCPDS}	$d_{theor.}$	d_{exp}	*hkl*	d_{JCPDS}	$d_{theor.}$	d_{exp}
100	9.12	9.119	9.038	002	1.86	1.859	1.860
110	5.29	5.265	5.260	500	1.824	1.823	1.830
200	4.56	4.559	4.559	321	1.823		
210	3.45	3.446	3.448	102	1.822	1.821	
101		3.443		330	1.755	1.755	1.762
300	3.04	3.039	3.036	411	1.754	1.755	
111		3.037		112		1.753	
201	2.88	2.881	2.882	420	1.724	1.723	1.730
220	2.63	2.632	2.640	202		1.721	1.722
310	2.53	2.529	2.533	510		1.637	1.643
211		2.528		501		1.637	
301		2.353		212	1.634	1.636	1.639
400		2.279	2.287	331	1.59	1.587	1.593
221	2.147	2.148	2.153	302		1.586	
320	2.097	2.092	2.099	421	1.566	1.563	1.570
311		2.091					
410	1.993	1.989	2.000				
401	1.947	1.943	1.949				

Note. d_{JCPDS} correspond to card 21-569; $d_{theor.}$ correspond to results calculated from parameters published by Olenkova *et al.* (4) ($a = 10.54$ Å, $c = 3.71$ Å, SG = $P6_3$).

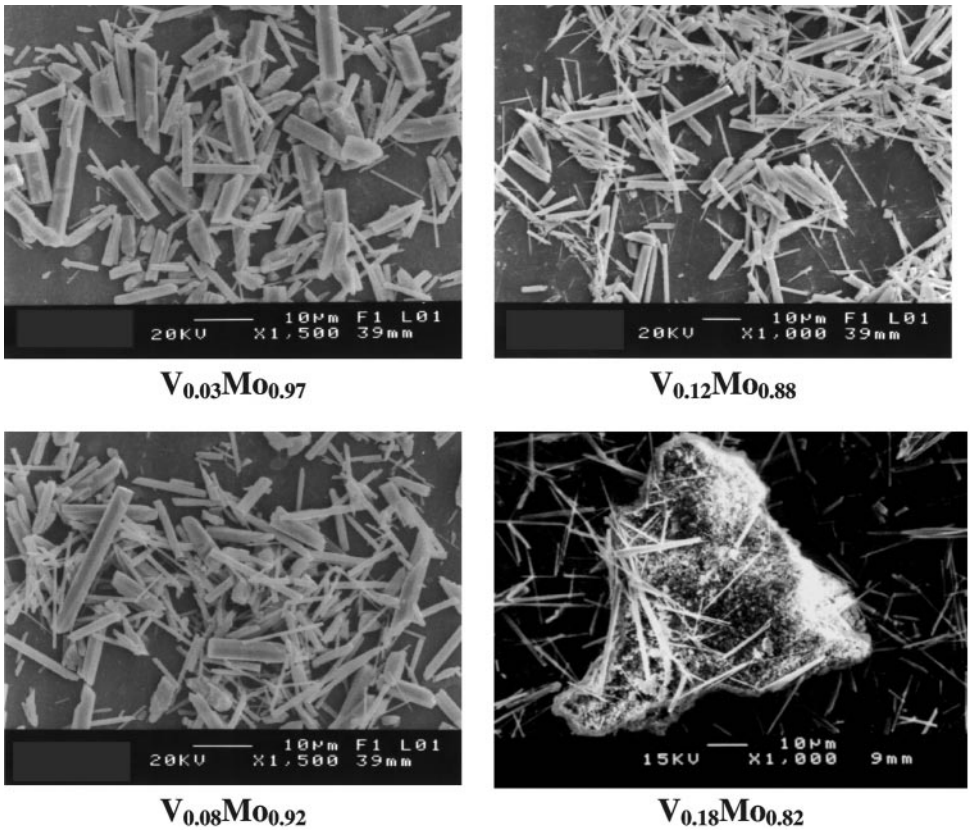

FIG. 3. SEM observation of the needle morphology of the precipitates: evolution of the particle size versus vanadium amount.

the needles. The larger the quantity of vanadium, the thinner the needles are. The precipitated samples have been investigated by EDX microanalysis. The results showed a variation of vanadium content between the surface and the center of the needles; the surface is 30% richer in vanadium than the center. As a consequence, one can assume that vanadium atoms orient the needles growing along the *c*-axis.

Although the X-ray diffraction analysis patterns show a pure single h-MoO_3-like phase, the precipitated samples are not pure MoO_3. Apart from vanadium, molybdenum, and oxygen, the precipitates contain other elements. The samples were analyzed by TGA–DTA, and the results showed three weight losses (Fig. 5a): the first one, around 100–150°C, corresponds to an endothermic loss of adsorbed water, while the second, around 270–300°C, corresponds to the elimination of ammonium nitrates formed during the synthesis. The last weight loss occurs during an exothermic phenomenon, which corresponds to the decomposition of the metastable hexagonal h-MoO_3-like phase into an orthorhombic MoO_3 phase and an intermediate compound (27), e.g., $V_9Mo_6O_{40}$ (31–35). The hexagonal structure is metastable because its decomposition into α-MoO_3 and $V_9Mo_6O_{40}$ is not reversible. This point has already been observed by Guidot *et al.* (27).

By processing our samples for 24 hours at 350°C, we minimized the total weight loss, but the weight loss that occurs during the phase decomposition can neither be minimized nor avoided without transforming the phase (Fig. 5b). EDX analyses of these processed samples have shown a homogenization of vanadium content in the needles; the surface and the center vanadium contents are then the same.

The results of mass spectrometry showed the presence of gases such as NH_3, N_2, NO, N_2O, NO_2, and H_2O during the phase decomposition under an argon flux. This observation confirms the presence of ammonium in the tunnels of the hexagonal structure, and allows us to use the same formula as Olenkova *et al.* (4), Hu and Davies (7), or Darriet and Gally (11): $A_xV_xMo_{1-x}O_3$ with $A = NH_4^+$.

The existence of the hexagonal vanadium–molybdenum oxide solid solution has been pointed out by DTA. The determination of the phase decomposition temperature versus vanadium content shows a stabilizing effect of vanadium (Fig. 6). This decomposition temperature increases, to reach a maximum at $T = 469$°C for $x = 0.12$. If the content of

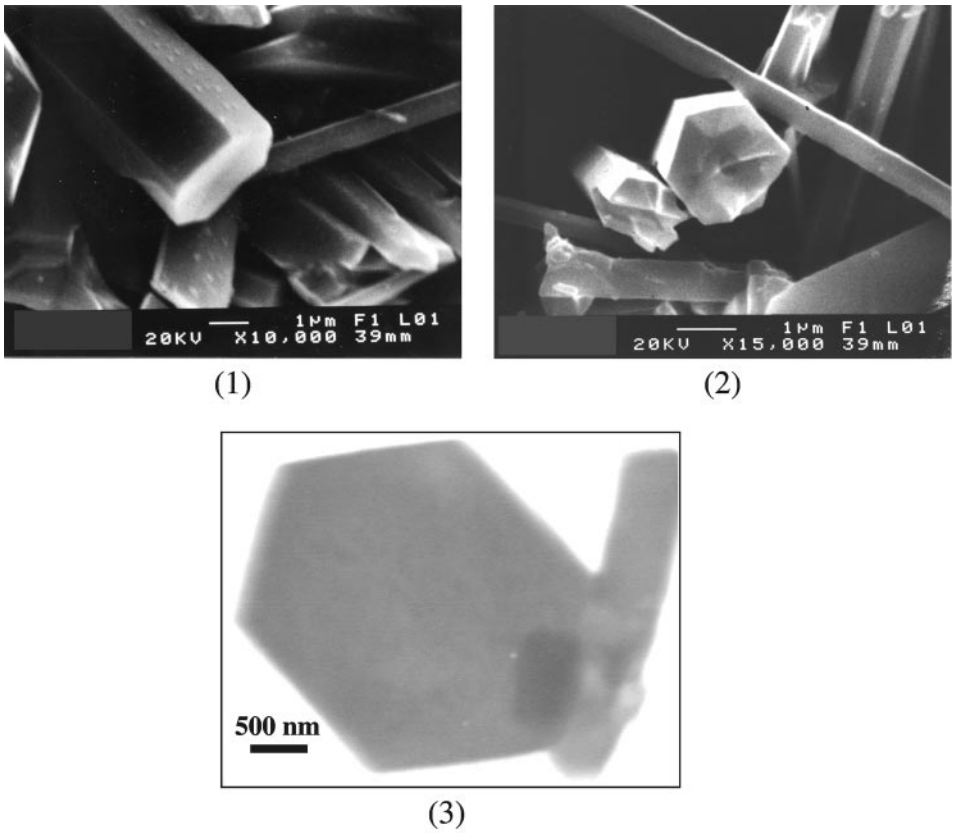

FIG. 4. SEM (1 and 2) and TEM (3) observations of the hexagonal section of the needles.

vanadium is increased over 0.13, the phase decomposition temperature decreases to reach a level at $T = 450°C$ for x greater than 0.20. This can be explained by a decrease of the vanadium content in the hexagonal phase, which is involved in the formation of the second phase ($V_9Mo_6O_{40}$). An EDX microanalysis has confirmed that point; beyond the solubility limit, the needles formed during the precipitating process contain less vanadium (Table 5). The consequence is a diminution of the hexagonal phase decomposition temperature.

The experimental weight loss of ammonium during the hexagonal phase decomposition was measured for all our samples. Figure 7 illustrates the variation of the experimental weight loss during the phase decomposition versus the value of x in the formula $(NH_4)_xV_xMo_{1-x}O_3$.

The curve shows three domains:

I. First, the experimental weight loss decreases upon addition of some vanadium; this may be explained by the presence of molybdenum vacancies, which implies the presence of ammonium cations to preserve the electric neutrality. The presence of vacancies in pure molybdenum oxide (without vanadium) has already been shown by Caiger *et al.* (15), and by Hu and Davies (30), in the case of vanadium-containing hexagonal molybdates. The fact that the weight loss decreases with the addition of vanadium implies that vanadium first fills the molybdenum vacancies. This can be summarized by the model $(NH_4)_{6y}Mo_{1-y}\square^{Mo}{}_yO_3$ when no vanadium is present in the structure, and $(NH_4)_{6y-5x}V_xMo_{1-y}\square^{Mo}{}_{y-x}O_3$ when introducing vanadium.

II. When all the molybdenum vacancies are filled, e.g., when $x = y$ in our model, the experimental weight loss increases; there is more ammonium in the structure. This can be explained by the fact that vanadium atoms enter the hexagonal structure by substituting molybdenum, thus giving the formula $(NH_4)_xV_xMo_{1-x}O_3$.

III. On the third part of the graph, the experimental weight loss decreases. The limit of solubility of vanadium in the hexagonal h-MoO_3 structure has been reached. A second phase appears, so that the ratio of hexagonal phase in the system decreases; as a consequence, the quantity of ammonium cations in the system is smaller, and the weight loss is lower too.

The introduction of vanadium in the hexagonal structure of MoO_3 seems to modify the X-ray diffraction pattern (peak apparitions, and peak shifts) (Fig. 2); however, we still exclusively observe the hexagonal structure. All the

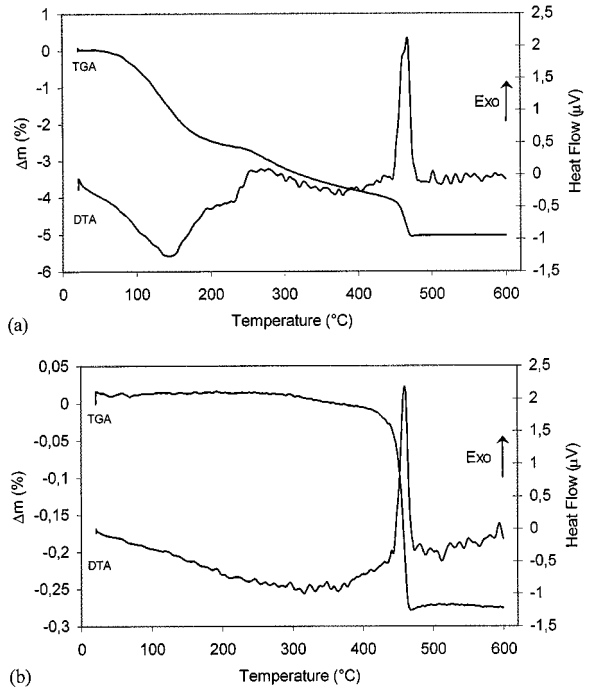

FIG. 5. TGA–DTA (3°C/minute, air) of a sample $V_{0.09}Mo_{0.91}$ ($m \approx 22$ mg), with the h-MoO_3-like structure, (a) before processing and (b) processed during 24 hours at 350°C.

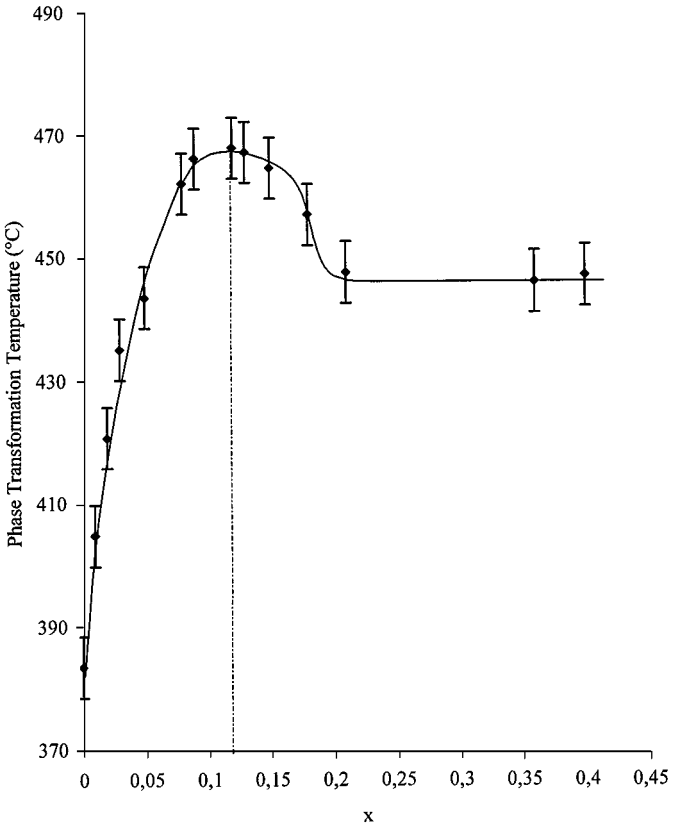

FIG. 6. Evolution of the decomposition temperature of the hexagonal phase to the orthorhombic one, as a function of the content of vanadium x.

diffraction diagram can be indexed in the hexagonal symmetry, with the space group $P6_3$ (Fig. 8). This result is in agreement with the JCPDS card no. 81-2414.

With this (*hkl*) identification, the parameters of all our samples were refined, and the variation of a and c as a function of the content of vanadium x was determined (Fig. 9). These curves show that the parameters a and c do not vary in the same way. With the first addition of vanadium (small x), while c decreases, a starts increasing and then follows the same trend as c. This phenomenon is unexpected, as we were predicting a decrease of both parameters a and c, because of the smaller size of vanadium V^{5+} ions ($r = 0.59$ Å) regarding the size of molybdenum Mo^{6+} ions ($r = 0.62$ Å).

But if we compare this result to the variation of the weight loss versus the content of vanadium (Fig. 7), we can observe that the increase of a corresponds to a decrease of the quantity of ammonium ions in the tunnels of the hexagonal structure. This observation is not consistent with the model: if there are fewer ammonium ions, the parameter a should decrease. A possible explanation for our observation may be that the NH_4^+ ions have positive electrostatic charges which are able to disorganize and to attract the oxygen atoms present at the periphery of the tunnels.

Similar results have been published. Guido, Arnaud and Germain (27) showed an increase of a when introducing small amounts of vanadium in the h-MoO_3 structure; Hu and Davies (7) found lower lattice parameters with potassium in the tunnels ($K_{0.13}(V_{0.13}Mo_{0.87})O_3$, $a = 10.481$ Å, $c = 3.701$ Å) than without ($(V_{0.13}Mo_{0.87})O_{2.935}$, $a = 10.593$ Å, $c = 3.694$ Å); Dupont (35) also made the hypothesis that the presence of monovalent cations may reduce the value of parameter a. As a consequence, the presence of ammonium in the tunnels will contract the lattice, and the a parameter will decrease. In contrast, less ammonium will result in an increase of the parameter a. The variation of the parameter c is only due to the vanadium, because the ammonium cations in the tunnels do not have any neighbors along the c axis (Fig. 1).

When we introduce vanadium in our system, we first fill the molybdenum vacancies, so according to the formula

TABLE 5
Comparison of Vanadium Content x in V_xMo_{1-x}, Measured out by SAA (x in the Sample) and by EDX (x in the Needles)

x in the sample	x in the needles
0.03	0.03
0.12	0.11
0.40	0.08

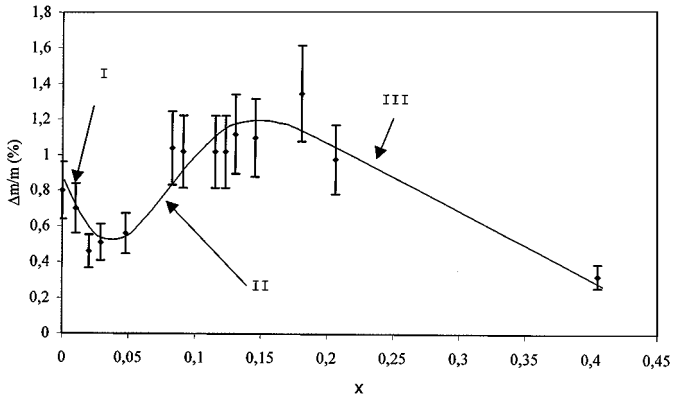

FIG. 7. Variation of the experimental weight loss during the phase transformation versus x in $(NH_4)_xV_xMo_{1-x}O_3$.

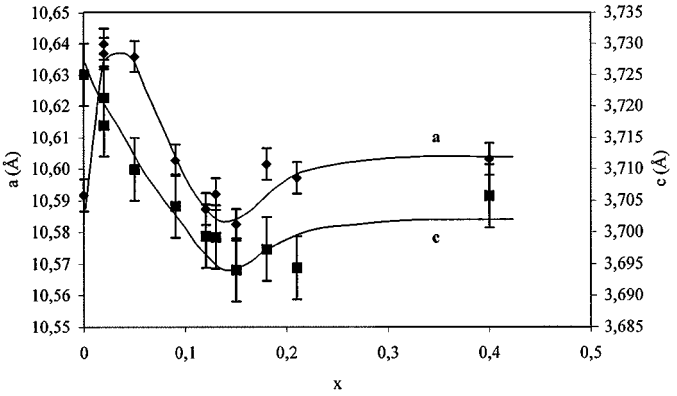

FIG. 9. Evolution of the a and c parameters as a function of the vanadium content, x, in our samples, thermally treated 24 hours at 350°C.

$(NH_4)_{6y-5x}V_xMo_{1-y}\square^{Mo}{}_{y-x}O_3$, the quantity of ammonium decreases, and the parameter a increases.

When all the vacancies are filled, vanadium atoms substitute molybdenum, and the quantity of ammonium in the tunnels increases to preserve electroneutrality, in agreement with the formula $(NH_4)_xV_xMo_{1-x}O_3$. The consequence is a decrease of the parameter a to reach a minimum for $x = 0.13$.

For x greater than 0.13, parameters a and c increase. This can be explained by XRD and EDX results which have shown that the system is not monophased any longer, and that the quantity of vanadium content in the hexagonal needles decreases to form the phase $V_9Mo_6O_{40}$. As a consequence, it is normal to observe an increase of a and c parameters.

The thermally purified samples have been analyzed by infrared spectrometry. The infrared spectra have been recorded from 4000 to 400 cm^{-1}, but the more interesting range extends from 1200 to 400 cm^{-1}. We can observe three absorption bands in these spectra, and we can see that these IR spectra show a mobile band at 980 cm^{-1}, which shifts toward higher wavelengths when the content of vanadium increases. According to Grussenmeyer (36), this band is due to vibrations of metal oxygen bonds $M=O$. If we plot the variation of this band position as a function of x, the content of vanadium in our samples, one can observe that the wavelength of this band increases until $x = 0.13$; over this value the band does not shift any more (Fig. 10).

If we compare this result with those obtained for the weight loss, the TDA, and the XRD analyses, one can conclude that the existence of the solid solution $(NH_4)_xV_xMo_{1-x}O_3$ with the MoO_3 type hexagonal structure is limited to $x = 0.13 \pm 0.01$.

4. CONCLUSION

In our study, we have pointed out the existence and the limit of the vanadium solid solution in the hexagonal molybdenum oxide. Our samples have been obtained by a soft chemistry method; the precipitates are well crystallized with

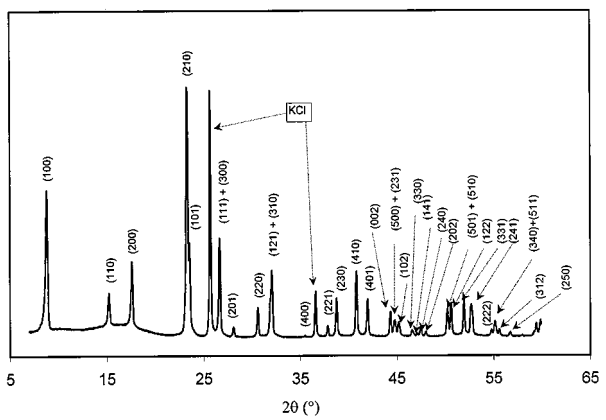

FIG. 8. X-ray diffraction pattern corresponding to $V_{0.12}Mo_{0.88}$ oxide with the hexagonal structure.

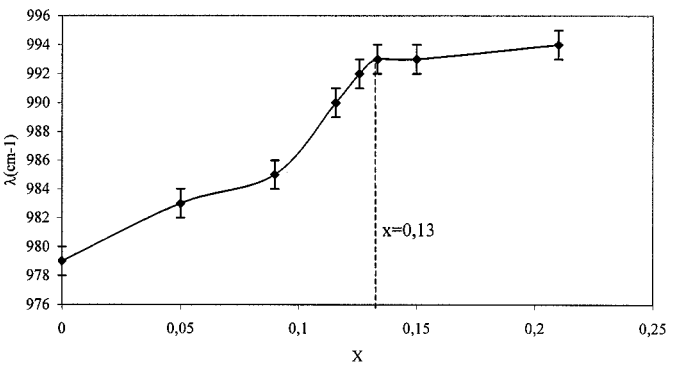

FIG. 10. Evolution of the wavenumber λ in the IR spectra as a function of x, the vanadium content in the samples.

a hexagonal h-MoO_3 type structure, and with a needle morphology with a hexagonal cross section.

There are two domains in this solid solution depending on the amount of vanadium introduced during the precipitating step: first the insertion of vanadium fills the molybdenum vacancies of the h-MoO_3 structure according to the formula $(NH_4)_{6y-5x}V_xMo_{1-y}\square^{Mo}_{y-x}O_3$, and then vanadium substitutes molybdenum according to the formula $(NH_4)_xV_xMo_{1-x}O_3$. According to these two models, the quantity of ammonium ions changes: first it decreases, and then it increases. Because of its positive electrostatic charge, the ammonium ions produces in the first domain an *a* parameter increase when the ammonium amount decreases, and in the second domain an *a* parameter decrease when the ammonium amount increases.

All the analytical methods have shown that the solubility limit of vanadium in h-MoO_3 is obtained for $x = 0.13 \pm 0.01$, so that the maximum composition of this solid solution is $(NH_4)_{0.13}V_{0.13}Mo_{0.87}O_3$.

Beyond this solid solution limit, a second phase ($V_9Mo_6O_{40}$) is formed during the precipitation. This formation occurs with a diminution of vanadium content in the hexagonal structure. As a consequence, the phase decomposition temperature decreases, and parameters *a* and *c* increase.

ACKNOWLEDGMENTS

The authors thank the Elf Atochem group for sponsorship. We also thank L. Datas and J. Sarrias for the microscopy analysis.

REFERENCES

1. G. Anderson and A. Magneli, *Acta Chem. Scand.* **4,** 793 (1950).
2. L. Kihlborg, *Ark. Kemi* **21,** 357 (1963).
3. E. M. McCarron, III, *J. Chem. Soc., Chem. Commun.* 336 (1986).
4. I. P. Olenkova, L. M. Plyasova, and S. D. Kirik, *React. Kinet. Catal. Lett.* **16**(1), 81 (1981).
5. ICDD, PCPDFWIN v. 2.00, JCPDS-International Center for Diffraction Data, 1998.
6. M. Figlarz, *Prog. Solid State Chem.* **19,** 1 (1989).
7. Y. Hu and P. K. Davies, *J. Solid State Chem.* **105,** 489 (1993).
8. I. P. Olenkova, D. V. Tarasova, G. N. Kustova, G. I. Aleshina, and E. L. Mikhailenko, *React. Kinet. Catal. Lett.* **9**(2), 221 (1978).
9. T. P. Feist and P. K. Davies, *Chem. Mater.* **3,** 1011 (1991).
10. J. M. Tatibouet and J. E. Germain, *C.R. Acad. Sci. Paris, Sér. C* **290,** 321 (1980).
11. B. Darriet and J. Gally, *J. Solid State Chem.* **8,** 189 (1973).
12. A. Ch. Gurlo and M. I. Ivanovskaya, *Inorg. Mater.* **34**(12), 1237 (1998).
13. E. M. McCarron, III, D. M. Thomas, and J. C. Calabrese, *Inorg. Chem.* **26,** 370 (1987).
14. B. Krebs and I. Paulat-Böschen, *Acta Crystallogr. B* **32,** 1697 (1976).
15. N. A. Caiger, S. Crouch-Baker, P. G. Dickens, and G. S. James, *J. Solid State Chem.* **67,** 369 (1987).
16. J. Guo, P. Zavalij, and M. S. Whittingham, *J. Solid State Chem.* **117**(2), 323 (1995).
17. A. Bielanski and M. Najbar, *Appl. Catal. A: Gen.* **157,** 223 (1997).
18. J. Tichy, *Appl. Catal. A: Gen.* **157,** 363 (1997).
19. R. Burch and R. Swarnakar, *Appl. Catal.* **70,** 129 (1991).
20. A. Bielanski and A. Inglot, *Bull. Acad. Pol. Sci.* **22**(9), 773 (1974).
21. J. E. Germain and J. C. Peuch, *Bull. Soc. Chim. Fr.* **No. 6,** 1844 (1969).
22. T. V. Andrushkevich, *Catal. Rev.-Sci. Eng.* **35**(2), 213 (1993).
23. R. M. Munch and E. D. Pierron, *J. Catal.* **3,** 406 (1964).
24. L. M. Plyasova, L. P. Solov'eva, G. N. Kryukova, and T. V. Andrushkevich, *Kinet. Katal.* **31**(6), 1430 (1990).
25. J. Tichy, J. Kustka, and J. Machek, *Collect. Czech. Chem. Commun.* **48,** 698 (1983).
26. T. G. Kuznetsova, G. K. Boreskov, T. V. Andrushkevich, Yu. A. Grigorkina, N. G. Maksimov, I. P. Olenkova, L. M. Plyasova, and T. P. Gorshkova, *React. Kinet. Catal. Lett.* **19**(3–4), 405 (1982).
27. J. Guidot, Y. Arnaud, and J. E. Germain, *Bull. Soc. Chim. Fr.* **No. 5–6** (I-209), 217 (1980).
28. Y. Hu, P. K. Davies, and T. P. Feist, *Solid State Ionics* **53–56,** 539 (1992).
29. L. M. Plyasova, S. D. Kirik, and I. P. Olenkova, *J. Struct. Chem.* **23**(4), 590–593 (1982).
30. Y. Hu and P. K. Davies, *J. Solid State Chem.* **119,** 176 (1995).
31. A. Bielanski, K. Dyrek, J. Pozniczek, and E. Wenda, *Bull. Acad. Pol. Sci.* **19**(8), 507 (1971).
32. R. H. Jarman, P. G. Dickens, and A. J. Jacobson, *Mater. Res. Bull.* **17,** 325 (1982).
33. C. T. Slade, A. Ramanan, J. M. Nicol, and C. Ritter, *Mater. Res. Bull.* **23,** 647 (1988).
34. K. Ruth, R. Kieffer, and R. Burch, *J. Catal.* **1975,** 16 (1998).
35. L. Dupont, Thesis, Université de Picardie, France, 1997.
36. J. Grussenmeyer, Thesis, Université de Lyon, France, 1978.